NASA TECHNICAL MEMORANDUM

NASA TM X-3164

NASA TM X-3164

(NASA-TM-X-3164) EXHAUST EMISSIONS OF A DOUBLE ANNULAR COMBUSTOR: PARAMETRIC STUDY (NASA) 44 p HC $3.75 CSCL 21B
N75-16645
Unclas
H1/25 09745

EXHAUST EMISSIONS OF A DOUBLE ANNULAR COMBUSTOR - PARAMETRIC STUDY

Donald F. Schultz
Lewis Research Center
Cleveland, Ohio 44135

NATIONAL AERONAUTICS AND SPACE ADMINISTRATION • WASHINGTON, D. C. • FEBRUARY 1975

1. Report No.	2. Government Accession No.	3. Recipient's Catalog No.
NASA TM X-3164		

4. Title and Subtitle	5. Report Date
EXHAUST EMISSIONS OF A DOUBLE ANNULAR COMBUSTOR - PARAMETRIC STUDY	February 1975
	6. Performing Organization Code
7. Author(s)	8. Performing Organization Report No.
by Donald F. Schultz	E-8084
	10. Work Unit No.
9. Performing Organization Name and Address	505-04
Lewis Research Center National Aeronautics and Space Administration Cleveland, Ohio 44135	11. Contract or Grant No.
	13. Type of Report and Period Covered
12. Sponsoring Agency Name and Address	Technical Memorandum
National Aeronautics and Space Administration Washington, D.C. 20546	14. Sponsoring Agency Code

15. Supplementary Notes

16. Abstract

A parametric study of exhaust emissions was performed with a full-scale double-annular ram-induction combustor designed for Mach 3.0 cruise operation. Emissions of oxides of nitrogen, carbon monoxide, unburned hydrocarbons, and smoke were measured over a range of combustor operating variables including reference velocity, inlet air temperature and pressure, and exit average temperature. An equation is provided relating oxides of nitrogen emissions as a function of the combustor, operating variables. ASTM Jet-A fuel was used for these tests. A small effect of radial fuel staging on reducing exhaust emissions (which were originally quite low) was demonstrated.

17. Key Words (Suggested by Author(s))	18. Distribution Statement
Jet engine; Combustor; Annular combustor; Exhaust emissions; Double annular combustor	Unclassified - unlimited STAR category 25 (rev.)

19. Security Classif. (of this report)	20. Security Classif. (of this page)	21. No. of Pages	22. Price*
Unclassified	Unclassified	44	$3.25

* For sale by the National Technical Information Service, Springfield, Virginia 22151

EXHAUST EMISSIONS OF A DOUBLE ANNULAR COMBUSTOR - PARAMETRIC STUDY

by Donald F. Schultz

Lewis Research Center

SUMMARY

A parametric exhaust emissions study was performed with a full-scale double-annular ram-induction combustor designed for Mach 3.0 cruise operation. Emissions of oxides of nitrogen, carbon monoxide, unburned hydrocarbons, and smoke were measured as a function of combustor operating variables including reference velocity, inlet total pressure, temperature, and exit average temperature. An empirical equation is provided relating oxides of nitrogen emissions to inlet temperature and pressure, reference velocity, and exit average temperature. ASTM-Jet A fuel was used for all tests. Test conditions ranged from 20- to 62-newton-per-square-centimeter inlet total pressure, 585 to 895 K inlet temperature, 24- to 48-meter-per-second reference velocity, and 815 to 1475 K exit average temperature. In addition, emissions data were obtained at a simulated engine idle point of 41-newton-per-square-centimeter inlet total pressure, 480 K inlet temperature, 31-meter-per-second reference velocity, and a fuel-air ratio range of 0.008 to 0.012. This operating condition was selected as representative of the idle operation of a high pressure ratio turbofan engine. These idle performance tests were conducted to illustrate the degree of emission reduction that could be obtained with radial fuel staging.

INTRODUCTION

A parametric study was made of the exhaust emissions of a double-annular ram-induction combustor. Previous studies covering the performance of the double-annular combustor have included some data on exhaust pollutant levels (ref. 1). Other recent work with an annular combustor has demonstrated the effect of various changes in combustor operating conditions on the levels of exhaust pollutants (ref. 2). However, these two studies have not covered wide enough ranges of operating conditions to determine with a high degree of certainty the effect of each operating variable on emissions. A comparison of the data of reference 2 with the emissions measured from the double-annular combustor of reference 1 indicate emission levels are a function of the specific combustor designs.

The purpose of the parametric tests reported herein was to evaluate emissions of the double-annular combustor more completely than had been done previously, and to determine the effect of each operating variable on the level of emitted gaseous pollutant. These tests were conducted using the double-annular ram-induction combustor designed for operation at flight speeds up to Mach 3. In these tests the inlet-air pressure was varied from 20 to 62 newtons per square centimeter, the inlet-air temperature from 590 to 895 K, the reference velocity from 24 to 48 meters per second, and the combustor exit average temperature from 1250 to 1475 K. In addition, some data were obtained at a simulated engine idle condition comparable to that of a high pressure ratio turbofan engine. These data were taken to illustrate the effect of radial fuel staging and fuel-air ratio on idle emissions.

Appendixes A to D give details concerning reported symbols, combustor design, instrumentation, and calculations. The test facility used is described in reference 3.

APPARATUS

This investigation was conducted using a double-annular ram-induction combustor designed for Mach 3.0 cruise operation. Figure 1 shows a cross-sectional view of the combustor consisting of two concentric, but separate annular combustion zones. This particular arrangement allows for the firing of either or both annuli during engine idle operation. Performance tests of this combustor at idle conditions have been reported in reference 1. No modifications were made to the combustor while conducting the test program. The only changes made were in the size of simplex fuel nozzles . Three different sets of fuel nozzles (64 in each set) were interchanged to maintain a high fuel injection differential pressure at every operating condition. Variations in fuel flow rate with nozzle differential pressure for the three types of fuel nozzles are shown in figure 2. A more detailed description of this combustor is given in appendix B.

PROCEDURE

In these tests inlet air pressure was varied from 20 to 62 newtons per square centimeter, inlet air temperature from 590 to 895 K, reference velocity from 24 to 48 meters per second, and combustor average exit temperature from 1250 to 1475 K with some points with combustor average exit temperature as low as 815 K. Some data were taken at a simulated engine idle condition comparable to that of a high compression ratio turbojet engine. These data have average exit temperatures as low as 765 K. Table I outlines the range of test points taken.

RESULTS AND DISCUSSION

Table II is a list of test data covering all the conditions tested including the simulated engine idle points. ASTM Jet-A fuel was used for all tests. The design maximum average exit temperature of 1475 K was obtained at all conditions except at a condition of lowest reference velocity at the highest inlet air temperature tested. No effort was made to improve the exit temperature distribution other than selecting a set of simplex fuel nozzles which best fit the required fuel flows since a very low fuel nozzle differential pressure will usually increase pattern factor and decrease combustion efficiency.

General Combustor Performance

The combustor performed satisfactorily with the exception of minor erosion of turning vanes and warpage of some long center scoops. This testing program accumulated 46.7 hours of combustor burn time.

Combustion efficiency by thermocouple measurement. - The combustion efficiency was found to vary from 96 to 102 percent for all data points with an inlet air temperature greater than 580 K. Some of the engine idle data ranges down to 90 percent combustion efficiency.

Total pressure loss. - Figure 3 shows combustor total pressure loss (which includes the diffuser and combustor pressure loss) as a function of diffuser inlet Mach number. Most of the data presented is at a fuel-air ratio of 0.0258 though one isothermal data point is provided for reference. This figure covers the reference velocity range of 24 to 48 meters per second. The combustor design reference velocity was 32 meters per second, which gave a resulting total pressure loss of 5.8 percent.

Exit temperature parameters. - Figure 4 shows the exit temperature parameters of pattern factor, stator factor, and rotor factor (which are defined in appendix D), against inlet air temperature at a constant exit average temperature of 1475 K and 62-newton-per-square-centimeter inlet total pressure. (The temperature profile used to compute stator and rotor factor is shown in fig. 5.)

Comparing figures 4(a) to (c) shows that the exit temperature parameters are not reference velocity dependent. Figures 4(a) and (b) have curves of similar form which show the same kind of relation of either pattern factor or stator factor to inlet air temperature. Stator factor was always equal to or greater than pattern factor at the same operating condition. Since average exit temperature is constant, these figures also show that pattern and stator factors generally increase with increasing combustor average temperature rise as inlet air temperature decreases.

Figure 4(c) is somewhat unusual in that the opposite trend is evident. Increasing combustor temperature rise resulted in decreasing the rotor factor as is shown in figure 6. Figure 5, a plot of variation of exit average radial temperature profile with combustor average temperature rise, shows that, at high temperature rises, the exit average temperature profile deviates less from the ideal profile than at low temperature rises.

Exhaust Emissions

The exhaust emissions of oxides of nitrogen (NO_x), carbon monoxide (CO), unburned hydrocarbons, and smoke were measured. Gas sample validity was determined by computing a fuel-air ratio based on the exhaust products of carbon monoxide, carbon dioxide, and unburned hydrocarbons. This calculated fuel-air ratio was then compared to the actual metered fuel-air ratio. A ±5 percent agreement was required for good sample agreement. This comparison determines a FARR (fuel-air ratio ratio) value which is defined in appendix D.

NO_x emissions. - NO_x emissions have been found to be a function of inlet air humidity, pressure, temperature, reference Mach number, and exit temperature as reported in reference 2. The following correlation using a single-annular ram-induction combustor was derived:

$$NO_x(H, \theta, M, P) = NO_{x(std)}(0.1)e^{-19H}e^{1.14(\theta-1)}M^{-1}P^{0.5}\alpha \tag{1}$$

where $NO_{std} = 0.64 \pm 0.03$ and M is reference Mach number.

As the present study was made at constant reference velocity rather than constant reference Mach number as in reference 2, the following expression was derived for these data:

$$NO_{x_2} = NO_{x_1}\left(\frac{V_{ref_2}^{-1.42}T_{4_2} + 1.26\,V_{ref_2} - 105.5}{V_{ref_1}^{-1.42}T_{4_1} + 1.26\,V_{ref_1} - 105.5}\right)\frac{P_2^{1.33-5.93\times10^{-4}T_{4_2}}}{P_1^{1.33-5.93\times10^{-4}T_{4_1}}}$$

$$\times\, e^{\left[7.8\times10^{-7}\left(V_{ref_2}+V_{ref_1}\right)\left(T_{4_2}+T_{4_1}\right)+1.0\right](\theta_2-\theta_1)+2.61\times10^{-3}\left(T_{4_2}-T_{4_1}\right)-19(H_2-H_1)} \tag{2}$$

This equation provides agreement within ±4.8 percent standard deviation over the range of conditions tested. By substituting a set of convenient standard conditions for V_2, P_2, T_{3_2} and T_{4_2} such as

$V_{ref(std)}$ = 24 meters per second

P_{std} = 10.13 newton per square centimeter (1 atm)

$T_{3(std)}$ = 288 K (standard temperature)

$T_{4(std)}$ = 1475 K

for each known data point into this equation a $NO_{x(std)}$ number can be computed. Using 44 data points (all points with FARR values within 1.0±0.05), $NO_{x(std)}$ emission index value was determined to be 0.832 gram per kilogram of fuel with a standard deviation of 0.040. Figure 7 verifies the equation agreement. In this figure the actual NO_x value is ratioed to the calculated NO_x value as determined by using the following equation, which is the previous equation with standard conditions substituted for the V_1, P_1, T_{3_1}, and T_{4_1} terms. Thus;

$$NO_x = +4.9 \times 10^{-3} \left(105.5 - T_4 V_{ref}^{-1.42} - 1.26 V_{ref}\right) P^{\left(1.33-5.93\times10^{-4} T_4\right)}$$

$$\times e^{\left[7.8\times10^{-7}\left(V_{ref}+24\right)\left(T_4+1475\right)+1.0\right](\theta-1)+2.6\times10^{-3} T_4 - 3.86 - 19H} \qquad (3)$$

These equations are combustor geometry dependent and, therefore, one would expect some variations in results when scaling combustors of this type or when analyzing combustors of an entirely different type.

The variation in NO_x due to inlet air humidity was not evaluated as relatively dry air was used for all tests and no means of controlling inlet air humidity was available. Inlet air humidity was believed to be about 0.003 ±0.002 gram of water per gram of dry air.

Figures 8 to 10 are typical figures showing the effects of inlet air temperature, exit temperature, reference velocity, and inlet total pressure on NO_x emissions. All data points plotted which fall outside the ±5 percent band are tailed.

Figures 8 to 10 confirm the NO_x emission trends reported elsewhere (refs. 2, 4, and 5); namely, that NO_x increases exponentially as inlet-air temperature, and to a lesser degree as exit average temperature increases and decreases with increasing reference velocity. Also NO_x increases with increasing combustor inlet total pressure. The ranges of the operating condition variables were chosen to be as representative of actual gas turbine engine conditions as was possible. The greatest exception taken was the range of pressures tested. A value of 62 newtons per square centimeter was the maximum pressure available in test facility. A more accurate determination of the effect of pressure on NO_x should be determined from data obtained in test facilities capable of operating at high pressures.

Equations (2) and (3) should only be used for predicting oxides of nitrogen exhaust emissions at operating conditions within the data region from which the equations were derived. This is especially true with pressure. Also these equations are geometry dependent in that they may not hold true for double annular combustors of significantly different size or for combustors of different design such as the single-annular type used in equation (1). However, the basic trends appear to be similar to those obtained with other combustor types.

Carbon monoxide emissions. - As expected CO emissions decreased with increasing inlet air temperature, increasing exit temperature, and decreasing reference velocity. Figure 11 shows the reference velocity and inlet air temperature effects on CO emissions while figure 12 shows the exit temperature effect. Also shown in figure 12 is the absence of an inlet pressure effect over the range of test pressures available. That is, for the same combustor exit temperature the CO emissions indices for 20.7 and 62 newtons per square centimeter were identical within experimental error.

Unburned hydrocarbon emissions. - Unburned hydrocarbon emissions index remained below 1 gram per kilogram fuel for all data except those points with an exit average temperature below 950 K. The highest unburned hydrocarbon emissions index was 4.7 grams per kilogram of fuel at a condition of 62-newton-per-square-centimeter inlet total pressure, 590 K inlet air temperature, 31.4-meter-per-second reference velocity, and 814 K exit average temperature.

These values were so low that no realistic determination can be made of the emission trends with operating condition. The inherent experimental errors in determining the values of unburned hydrocarbon emissions were high due to the very low levels of unburned hydrocarbons. It is usually assumed that the trends in unburned hydrocarbon emissions are similar to those of carbon monoxide emissions except that the values are much lower.

Smoke emissions. - A limited amount of smoke data were obtained. The highest smoke number 16.5 was obtained at 590 K inlet air temperature, 62-newton-per-square-centimeter inlet total pressure, 24-meter-per-second reference velocity, and 1370 K exit average temperature. This is 18 percent below the value of 20 which is the acceptable maximum smoke number for combustors of this size (ref. 6). Figure 13 shows smoke number as a function of reference velocity at constant inlet pressure and exit temperature and the effect of increasing inlet air temperatures. Both of these curves reach minimum values near 32 meters per second, the design reference velocity of this combustor. Figure 14 shows the effect of exit average temperature, on two similar double annular combustors, holding reference velocity, inlet total pressure, and inlet temperature constant. Smoke number was found to decrease with increasing exit temperature over the range tested on both combustors.

Inlet total pressure had no effect on smoke number over the range of pressures tested (20 to 62 N/sq cm).

Engine Idle Exhaust Emissions

The idle emissions of the double-annular combustor were measured at an engine idle of 41-newton-per-square-centimeter inlet total pressure, 475 K inlet air temperature, 32-meter-per-second reference velocity: corresponding to that of a higher compression ratio turbofan engine to demonstrate the reduction in exhaust emissions that could be obtained by utilizing radial fuel staging. In radial fuel staging, fuel was supplied to only one annulus rather than to both as in the usual case at other engine conditions. As shown in figure 15(a), a combustion efficiency (determined by exhaust gas analysis), of 98.1 percent was obtained using radial fuel staging at an overall fuel-air ratio of 0.012. This is about one percentage point better than was obtained with fuel supplied to both annuli at the same fuel-air ratio. The lowest carbon monoxide and unburned hydrocarbon emissions occurred when radial fuel staging was employed as shown in figures 15(c) and (d). Interestingly, unburned hydrocarbon emissions reached minimum values with fuel flow only to the inner annulus while carbon monoxide emissions reached minimum values with fuel flow only to the outer annulus. Note that the resulting combustion efficiency was the same for combustion in either annulus.

Oxides of nitrogen emissions were higher for combustion in only one annulus than they were for combustion on both as would be expected by the higher local temperatures (the local fuel-air ratio is doubled when radial fuel staging is employed compared to combustion on both annuli). Interestingly, NO_x emissions were lower for combustion on the outer annulus only than for combustion on the inner annulus only. In any case the NO_x emissions index remains below a value of 3.1 grams per kilogram of fuel, over the range of engine idle fuel-air ratios tested.

SUMMARY OF RESULTS

A full-scale double-annular ram-induction combustor designed for Mach 3 cruise conditions was used in a parametric study to determine the effect of operating conditions on combustor performance and exhaust emissions. The following results were obtained:

1. NO_x emissions index values can be described as a function of combustor operating conditions, and a correlating equation is developed which fits the experimental data well within ±10 percent.

2. Smoke numbers were very low and reached a minimum of four at a 32-meter-per-second reference velocity, 62-newton-per-square-centimeter inlet pressure, 590 K inlet air temperature, and 1475 K exit temperature.

3. A maximum combustion efficiency of 98.1 percent was obtained by radial fuel staging at a simulated engine idle condition for a high pressure ratio fan engine operating at a 32-meter-per-second reference velocity, 41-newton-per-square-centimeter inlet pressure, 478 K inlet air temperature, and a fuel-air ratio of 0.012. This resulted from a reduction in carbon monoxide and unburned hydrocarbons which increased combustor efficiency by approximately 1 percent above the 97 percent value obtained without staging.

Lewis Research Center,
National Aeronautics and Space Administration,
Cleveland, Ohio, October 22, 1974,
505-04.

APPENDIX A

SYMBOLS

CO carbon monoxide

H humidity, g water/g dry air

M Mach number

NO_x oxides of nitrogen

P pressure

ΔP total pressure drop across combustor, $Pt_3 - Pt_4$

T temperature

ΔT temperature rise across combustor $T_{t_4} - T_{t_3}$

V velocity

α function of exit temperature

δ factor

$\bar{\delta}$ pattern factor

η combustion efficiency

θ ratio of inlet air temperature to 288 K (standard temperature)

Subscripts:

des design

j radial location

loc local (a single point)

max maximum

ref reference

rot rotor

stat stator

std standard

t	total
1	test condition one
2	test condition two
3	11.4 cm upstream of diffuser inlet
4	combustor exit

APPENDIX B

COMBUSTION DESIGN

Double-Annular Concept

The combustor used in this investigation is referred to as a double-annular ram-induction combustor. Constructing the combustion zone as a double annulus permits the reduction of overall combustor length while maintaining an adequate ratio of length to annulus height in each combustion zone. This double-annular feature allows a considerable reduction in length to be made over a single annulus with the same overall height.

However, individual control of the inner and outer annulus fuel systems of the double-annular combustion zone provides a useful method for adjusting the outlet radial temperature profile. This individual fuel control can be extended to include radial fuel staging which is useful at engine idle conditions.

Ram-Induction Concept

The ram-induction combustor differs from the more conventional combustors in that the compressor discharge air is allowed to penetrate into the combustion and mixing zones without diffusing to as high a static pressure as a conventional static pressure-fed combustor. The kinetic energy of the inlet air is thereby used to promote rapid mixing of air and fuel in the primary zone and diluent air and burned gases in the mixing zone. The airflow is efficiently turned into the combustor by two rows of vaned turning scoops that penetrate into the combustion zones.

A more detailed description of the ram-induction concept is found in reference 7.

Combustor Design Details

The double-annular ram-induction combustor including the diffuser section used for this investigation is shown in cross section in figure 1. Forward airflow spreaders in the diffuser split the inlet airflow into three passages leading into the combustor. These are the inner liner passage, the outer liner passage, and the center passage. About 50 percent of the airflow is ducted by shrouds surrounding the outside of both the outer and inner liners of the combustor. The high velocity airflow which is maintained from the diffuser inlet through this ducting is turned into the combustor burning zones by means of the scoops discussed previously. The first row of scoops supplies air to the primary zone while the second row supplies diluent air to the secondary zone.

Basic dimensions for this combustor are shown in figure 1. The diameters are essentially those of the combustor for the Pratt and Whitney Aircraft experimental supersonic transport engine (JTF 17 (ref. 8)). However, the diffuser-combustor overall length of the double-annular combustor is about 30 percent shorter than that used in the JTF 17 engine.

Photographs of the combustor are shown in figure 16. Figure 16(a) shows the downstream end with the two circumferential rows of scoops of the inner and outer liners and those of the center section. Figure 16(b) is a closeup of this same view showing more detail of the scoop arrangement. The fuel nozzles and associated swirlers are included, in this view along with the deflectors for cooling the inner and outer headplates. A side view of the combustor with the upstream diffuser airflow spreaders and inner exit transition liner added to the combustor is shown in figure 16(c). The notches in the airflow spreaders fit around the diffuser struts. The combustor is pin mounted through the struts using tangs attached to the inner and outer headplates that extend forward into the airflow spreaders.

Fuel nozzles. - Simplex fuel nozzles with radial inflow air swirlers were used for the investigation. Curves of total fuel flow for the combustor (sum of 64 nozzles) as a function of pressure drop across these nozzles is shown in figure 2.

Combustor design specifications. - The major items in the combustor design are tabulated in table III. The circumferential locations of combustor components such as scoops, fuel nozzles, and diffuser struts are shown in figure 17. The flow areas as distributed among the many openings (scoops, film cooling, swirlers, etc.) are shown in figure 18. The scoop discharge areas with length and width dimensions are listed in table IV.

APPENDIX C

INSTRUMENTATION

Measurement Methods

Measurements to determine combustor operation and performance were recorded by the Lewis Central Automatic Data Processing System (ref. 9). Control room readout instrumentation (indicating and recording) was used to set and monitor the test conditions and the operation of the combustor. Pressures were measured and recorded by the central Digital Automatic Multiple Pressure Recorder (DAMPR) and by strain-gage pressure transducers (ref. 10). Iron-constantan thermocouples were used to measure temperatures between 240 to 675 K, Chromel-Alumel thermocouples measured temperatures between 240 and 1560 K. High temperatures, 275 to 1920 K were measured with platinum plus 13 percent rhodium/platinum thermocouples. The indicated readings of all thermocouples were taken as true values of the total temperatures. The platinum plus 13 percent rhodium/platinum thermocouples were of the high-recovery aspirating type (ref. 11, type 6).

Airflow rates were measured by square-edged orifices installed according to ASME specifications. Fuel flow rates were measured by turbine flowmeters using frequency-to-voltage converters for readout and recording.

Instrumentation Stations

The locations of the combustor instrumentation stations are shown in figure 1. Inlet air temperature was measured by eight Chromel-Alumel thermocouples that were equally spaced around the inlet at station 3. Inlet air total pressure was measured by eight five-point total pressure rakes equally spaced around the inlet at station 3. The pressure rakes measured the total pressure profile at centers of equal areas across the inlet annulus. Static pressure at the inlet was measured by 16 wall static pressure taps with eight on the outer and eight on the inner walls of the annulus at station 3.

Combustor outlet total temperature and pressure at instrumentation station 4 were measured at 3° increments around the exit circumference. At each 3° increment, five temperature and pressure points were measured across the annulus. The water-cooled probe assembly containing the five temperature and pressure sensors is shown in figure 19. Three of these probes, each on an arm 120° apart, rotated 120° providing full coverage of the circumference. Water-cooled shields protected these probes when they were not in use at three fixed points in the exhaust stream. At these points, temperature and pressure were not measured. The probes were made of platinum-rhodium alloy where exposed to the hot exhaust gases. Also located at station 4 were eight wall static pressure taps.

Rotating gas samples were taken at station 4 using three five-point water-cooled probes which were attached to the same drum as the five-point total temperature and total pressure probes. A continuous sample was taken during each traverse. An analysis of the exhaust products was made at each 3° increment around the exit circumference.

APPENDIX D

CALCULATIONS

Combustion Efficiency by Thermocouple Measurement

Efficiency by thermocouple measurement was determined by dividing the measured temperature rise across the combustor by the theoretical temperature rise. The theoretical rise is calculated from the fuel-air ratio, fuel properties, inlet air temperature, and pressure, as well as the amount of water vapor present in the inlet airflow. The exit temperatures were measured with five-point traversing aspirated thermocouple probes and were mass-weighted for the efficiency calculation. The indicated readings of all thermocouples were taken as true values of the total temperatures. The mass-weighting procedure is given in reference 8. In each mass-weighted average, 585 individual exit temperatures were used.

Combustion Efficiency by Gas Analysis

Efficiency by gas analysis was determined by measuring the exhaust products of carbon dioxide, carbon monoxide, and unburned hydrocarbons. An analysis was made 39 times during each data point. The derived combustion efficiency was validated by determining the combustor fuel-air ratio from the exhaust analysis. The fuel-air ratio by gas analysis was divided by the metered fuel-air ratio. This ratio is called FARR in the data table (table II).

An additional check on gas sample validity was made on selected data points. For this check the remaining oxygen in the exhaust was measured. A fuel-air ratio was determined from this which was compared to the metered fuel-air ratio. The fuel-air ratio by oxygen measurement was divided by the metered fuel-air ratio. This ratio is called FARRO in the data table (table II).

FARR and FARRO values of 1.0 ± 0.05 were considered acceptable values. Nearly all data points fall in this range.

Reference Velocity and Diffuser Inlet Mach Number

Reference velocity V_{ref} for the combustor was computed from the total airflow, the maximum cross-sectional area between the inner and outer shroud (see table IV), and the diffuser inlet using total pressure and temperature. Diffuser inlet Mach number was calculated from the total airflow; the total temperature, and the static pressure measured at the diffuser inlet, and the inlet annulus area.

Total Pressure Loss

The total pressure loss $\Delta P/P_{t3}$ was calculated by mass-averaging total pressures measured upstream of the diffuser inlet and at the combustor exit. The total pressure loss, therefore, includes the diffuser loss.

Exit Temperature Profile Parameters

Three parameters of interest in evaluating the quality of exit temperature profile are considered. Figure 20 is a graphical explanation of these parameters. Figure 5 shows the desired exit temperature profile used to compute stator and rotor factor.

The exit temperature pattern factor $\bar{\delta}$ is one parameter which is defined as

$$\bar{\delta} = \frac{T_{t4(max)} - T_{t4}}{T_{t4} - T_{t3}}$$

where T_{t4} and T_{t3} are averages of temperatures measured at the exit and inlet, and where $T_{t4(max)} - T_{t4}$ is the maximum temperature occurring anywhere in the combustor exit plane minus the average exit temperature. The parameter is useful for preliminary screening, but it does not take into account the desired radial temperature profile for which the combustor was designed. The desired average radial distribution of temperature at the combustor exit plane is determined by the stress and cooling characteristics of the turbine. For purposes of evaluating the double-annular combustor, an exit radial temperature profile was selected for conditions that are typical of advanced engines.

The two other parameters take the design profile into account. These parameters are

$$\delta_{stat} = \frac{\left[T_{t4j(loc)} - T_{t4j(des)}\right]_{max}}{T_{t4} - T_{t3}}$$

$$\delta_{rot} = \frac{\left[T_{t4j} - T_{t4j(des)}\right]_{max}}{T_{t4} - T_{t3}}$$

where $\left[T_{t4j(loc)} - T_{t4j(des)}\right]_{max}$ for δ_{stat} is the maximum positive temperature difference between the highest local temperature at any given radius and the design temperature for that same radius (subscript j refers to any radial location in the radial temperature profile) and where $\left[T_{t4j} - T_{4j(des)}\right]_{max}$ for δ_{rot} is the maximum temperature difference between the average temperature at any given radius around the circumference and the design temperature for that same radius (see fig. 20). The term $T_{t4} - T_{t3}$ used in all three parameters is the average temperature rise across the combustor ΔT.

The parameter δ_{stol} is a measure of the quality of the exit temperature profile on the turbine stator, and δ_{rot} is a measure of the quality or the exit temperature profile on the turbine rotor.

Units

The U.S. customary system of units was used for primary measurements and calculations. Conversion to SI units (Systeme International d'Unités) is done for reporting purposes only. In making the conversion, consideration is given to implied accuracy and may result in rounding off the values expressed in SI units.

REFERENCES

1. Schultz, Donald: Modifications that Improve Performance of a Double Annular Combustor at Simulated Engine Idle Conditions. NASA TM X-3127, 1974.

2. Marchionna, Nicholas R.; Diehl, Larry A.; and Trout, Arthur M.: Effect of Inlet-Air Humidity, Temperature, Pressure, and Reference Mach Number on the Formation of Oxides of Nitrogen in a Gas Turbine Combustor. NASA TN D-7396, 1973.

3. Schultz, Donald F.; and Perkins, Porter J.: Effects of Radial and Circumferential Inlet Velocity Profile Distortions on Performance of a Short-Length Double-Annular Ram-Induction Combustor. NASA TN D-6706, 1972.

4. Sawyer, Robert F.: Atmospheric Pollution by Aircraft Engines and Fuels - A Survey. AGARD-AR-40, Advisory Group for Aerospace Research and Development, 1973.

5. Lipfert, F. W.: Correlation of Gas Turbine Emissions Data. ASME Paper 72-GT-60, Mar. 1972.

6. Environmental Protection Agency: Control of Air Pollution from Aircraft and Aircraft Engines - Emission Standards and Test Procedures for Aircraft. Federal Register, vol. 38, no. 136, pt. 2, Tuesday, July 17, 1973, pp. 19088-19103.

7. Chamberlain, John: The Ram Induction Combustor Concept. Presented at AIAA Third Propulsion Joint Specialist Conference, Washington, D.C., July 7, 1967.

8. Rusnak, J. P.; and Shadowen, J. H.: Development of an Advanced Annular Combustor. (PWA-FR-2832, Pratt & Whitney Aircraft.) NASA CR-72453, 1969.

9. Central Automatic Data Processing System. NACA TN 4212, 1958.

10. Mealey, Charles; and Kee, Leslie: A Computer-Controlled Central Digital Data Acquisition System. NASA TN D-3904, 1967.

11. Glawe, George E.; Simmons, Frederick S.; and Stickney, Truman M.: Radiation and Recovery Corrections and Time Constants of Several Chromel-Alumel Thermocouple Probes in High-Temperature, High-Velocity Gas Streams. NACA TN 3766, 1956.

TABLE I. - TEST CONDITIONS

Inlet air		Reference velocity, V_{ref}, m/sec			
Temperature, K	Pressure, N/cm^2	24	32	40	48
		Exit average temperature range, K			
590	20	---------	1250-1475	---------	---------
590	41	---------	1250-1475	---------	---------
590	62	1250-1475	815-1475	1250-1475	1250-1475
755	62	1250-1475	815-1475	1250-1475	1250-1475
890	62	1250	815-1475	1250-1475	1250-1475
475	41	---------	765-940	---------	---------

PRECEDING PAGE BLANK NOT FILMED

TABLE II. -

Run number	Model	Inlet-air conditions				Combustor operating conditions							
		Total pressure, N/cm^2	Total temperature, K	Airflow, kg/sec	Diffuser inlet Mach number	Reference velocity, V_{ref}, m/sec	Fuel-air ratio	Total pressure loss,	Average outlet temperature, K	Inlet fuel temperature, K	Fuel nozzle differential pressure, N/cm^2	Annulus supplied with fuel	Pattern factor
322	10-2	62.4	590	48.6	0.239	30.9	0.019	-----	1282	294	116	Both	0.312
323	10-2	61.8	586	49.0	.243	31.2	.023	-----	1416	293	180		.327
324	10-2	62.3	587	50.6	.249	31.9	.0252	-----	1476	292	222		.397
525	10A	62.3	586	48.9	.241	30.9	.0103	-----	967	298	33		.286
526		62.2	586	49.3	.244	31.2	.0155	-----	1149	298	79		.345
527		62.1	587	49.4	.245	31.4	.0188	-----	1264	297	119		.384
528		62.6	587	49.3	.242	31.0	.0223	-----	1383	297	167		.326
530		62.3	587	49.5	.242	31.3	.026	-----	1497	297	229		.352
560		62.6	588	38.0	.183	24.0	.0253	-----	1472	296	128		.377
568		61.8	756	39.1	.221	32.2	.0215	-----	1487	297	98		.334
572		62.5	758	49.6	.283	40.4	.0214	-----	1481	297	157		. .
576		61.9	761	58.6	.347	48.2	.0214	-----	1484	296	218		.347
579		62.3	590	62.3	.317	39.5	.0256	-----	1473	294	346		.419
594		61.7	760	29.8	.166	24.7	.0213	-----	1453	298	54		.274
691	10-2	41.4	585	33.8	.250	32.1	.0216	-----	1349	288	71		.241
695	10-2	20.4	578	16.6	.246	31.5	.026	-----	1464	286	24		.262
1339	10-RH3	40.1	479	42.8	.301	34.2	.0077	7.11	776	---	---	i.d.	.779
1342		40.9	477	40.9	.280	32.0	.0081	7.15	764	293	57	o.d.	.965
1343		40.7	478	40.6	.278	31.9	.0102	7.14	834		90		.900
1344		40.9	479	40.5	.277	31.8	.0123	7.13	904		129		1.050
1345		40.8	479	41.0	.281	32.2	.0081	7.13	783		56		.779
1346		40.8	477	40.8	.278	31.9	.0102	7.15	854		88	i.d.	.790
1347		41.1	477	40.8	.277	31.7	.0122	13.47	924		127	i.d.	.827
1348		62.4	590	74.3	.388	46.8	.019	13.46	1250	294	263	Both	.277
1349		62.3	593	74.4	.390	47.2	.0189	13.84	1250	295	263		.271
1350		62.4	589	74.9	.392	47.1	.0225	13.95	1360	295	382		.289
1351		62.4	588	75.2	.393	47.3	.0263	8.99	1477	294	534		.288
1352		62.5	588	62.5	.315	39.3	.0189	8.95	1243	296	185		.260
1353		62.1	586	61.3	.310	38.8	.0228	-----	1363	296	260		.280

[a]$\dfrac{NO_{x_a}}{NO_{x_c}} = \dfrac{NO_x\text{(actual)}}{NO_x\text{(calculated (from }NO_{x(std)}\text{))}}$

EXPERIMENTAL DATA

		Combustor performance characteristics										
Stator factor	Rotor factor	Combustor average temperature rise, K	Thermocouple combustion efficiency, percent	NO_x emission index, g/kg of fuel	HC emissions index, g/kg of fuel	CO emission index, g/kg of fuel	Smoke number	FARR	FARRO	Gas analysis combustion efficiency, percent	$NO_{x(std)}$	$\frac{NO_{x_a}}{NO_{x_c}}$ [a]
-----	-----	692	102.9	----	-----	----	3.0	----	----	----	----	-----
-----	-----	830	102.6	----	-----	----	5.2	----	----	----	----	-----
-----	-----	889	102.9	----	-----	----	2.0	----	----	----	----	-----
0.262	0.067	381	100.4	----	-----	----	4.6	----	----	----	----	-----
.322	.017	563	101.4	----	-----	----	9.5	----	----	----	----	-----
.334	.019	676	102.0	----	-----	----	4.5	----	----	----	----	-----
.292	.049	796	102.8	----	-----	----	6.8	----	----	----	----	-----
.316	.055	910	102.9	----	-----	----	3.8	----	----	----	----	-----
.339	.076	884	102.2	----	-----	----	13.8	----	----	----	----	-----
.306	.029	731	101.6	----	-----	----	1.0	----	----	----	----	-----
.286	.027	723	100.8	----	-----	----	3.0	----	----	----	----	-----
.301	.020	723	101.0	----	-----	----	6.8	----	----	----	----	-----
.381	.049	882	101.3	----	-----	----	7.0	----	----	----	----	-----
.231	.032	693	97.1	----	-----	----	3.0	----	----	----	----	-----
.241	.025	764	101.1	----	-----	----	2.7	----	----	----	----	-----
.262	.029	887	99.6	----	-----	----	1.8	----	----	----	----	-----
.914	.627	297	98.2	0.99	15.5	95.8	----	1.03	----	96.1	----	-----
.964	.374	287	90.7	1.81	17.1	71.0	----	1.01	0.95	96.6	----	-----
.899	.391	357	90.9	2.14	9.41	62.1	----	.98	.97	97.6	----	-----
1.05	.407	424	91.3	2.48	5.69	56.0	----	.95	1.00	98.1	----	-----
.910	.627	305	96.4	3.04	14.4	76.7	----	1.07	1.23	96.8	----	-----
.896	.598	376	96.3	3.06	7.96	68.2	----	1.02	----	97.6	----	-----
.916	.580	447	97.0	3.04	5.12	58.0	----	1.00	----	98.1	----	-----
.277	.055	659	98.3	4.29	.25	27.9	----	.95	1.00	99.3	0.853	1.025
.271	.053	657	98.2	4.09	.24	27.1	----	.95	1.03	99.3	.812	.975
.289	.036	772	98.6	4.0	.06	18.3	----	.97	1.02	99.6	.795	.955
.289	.027	888	98.9	4.11	.01	13.1	----	.97	1.00	99.7	.814	.978
.259	.054	656	98.1	4.48	.10	16.5	----	.97	1.03	99.6	.765	.919
.280	.035	777	98.3	4.57	.16	10.7	----	.96	1.00	99.7	.774	.930

TABLE II. - Continued.

Run number	Model	Inlet-air conditions				Combustor operating conditions							
		Total pressure, N/cm^2	Total temperature, K	Airflow kg/sec	Diffuser inlet Mach number	Reference velocity, V_{ref}, m/sec	Fuel-air ratio	Total pressure loss,	Average outlet temperature, K	Inlet fuel temperature, K	Fuel nozzle differential pressure, N/cm^2	Annulus supplied with fuel	Pattern factor
1354	10-RH3	62.2	588	63.0	0.319	39.8	0.026	9.43	1463	295	365	Both	0.297
1355		62.5	592	50.8	.251	32.3	.0186	5.74	1242	297	118		.225
1356		61.8	588	49.5	.246	31.6	.0226	5.66	1359	297	165		.270
1357		62.1	590	49.6	.246	31.6	.0265	5.74	1476	296	230		.281
1358		61.8	591	37.8	.186	24.3	.0188	3.49	1236	298	66		.215
1359		62.7	587	37.6	.181	23.6	.0224	3.30	1345	296	93		.269
1360		62.2	584	37.7	.182	23.7	.0265	3.39	1461	296	131		.283
1362		41.5	587	34.4	.255	32.5	.0182	6.39	1212	296	50		.201
1363		62.6	760	58.7	.341	47.6	.0144	9.91	1253	297	94		.132
1364		62.8	763	58.5	.339	47.5	.0180	9.92	1365	297	146		.156
1365		62.3	761	58.8	.344	48.0	.0216	10.25	1473	297	215		.166
1366		62.7	760	49.4	.280	40.1	.0140	6.72	1234	300	62		.150
1369		62.5	756	48.1	.272	39.0	.0183	6.64	1366	299	101		.145
1371		62.2	757	48.5	.276	39.5	.0220	6.77	1477	298	150		.162
1372		62.4	760	39.3	.220	32.1	.0179	4.33	1352	300	64		.138
1373		61.9	752	38.5	.216	31.4	.0222	4.52	1470	298	96		.164
1374		62.2	758	38.5	.216	31.5	.0147	4.30	1252	301	42		.142
1375		62.4	759	38.5	.215	31.4	.0223	4.34	1477	298	97		.162
1376		62.8	750	30.6	.167	24.5	.0212	2.67	1443	300	54		.182
1377	10-RH3	62.3	757	30.6	.169	25.0	.0224	2.75	1479	301	61		.183
1380		62.3	898	48.0	.303	46.4	.0147	7.95	1379	302	65		.195
1381		62.7	895	49.1	.306	46.9	.0179	7.93	1476	299	101		.184
1382		62.4	895	49.7	.312	47.8	.0106	8.01	1253	305	37		.201
1384		62.4	894	41.1	.253	39.5	.0180	5.56	1472	301	72		.169
1387		62.1	585	50.4	.248	31.8	.0144	5.42	1108	298	68		.195
1388		41.7	586	33.6	.248	31.7	.0197	5.98	1262	295	57		.233
1389		41.4	585	33.5	.249	31.8	.0230	5.93	1358	295	77		.296
1390		41.2	583	34.1	.253	32.3	.0263	6.12	1469	294	105		.317
1391		41.0	586	33.5	.251	32.1	.0196	5.97	1260	295	56		.235

[a] $\frac{NO_{x_a}}{NO_{x_c}} = \frac{NO_x(\text{actual})}{NO_x(\text{calculated (from } NO_{x(std)}))}$

EXPERIMENTAL DATA

Combustor performance characteristics												
Stator factor	Rotor factor	Combustor average temperature rise, K	Thermocouple combustion, efficiency, percent	NO_x emission index, g/kg of fuel	HC emissions index, g/kg of fuel	CO emission index, g/kg of fuel	Smoke number	FARR	FARRO	Gas analysis combustion efficiency, percent	$NO_{x(std)}$	$\frac{NO_{x_a}}{NO_{x_c}}$ [a]
0.297	0.027	875	98.3	4.63	0.03	8.6	----	0.96	1.00	99.8	0.784	0.942
.224	.057	650	98.4	5.37	.06	10.7	----	.96	1.02	99.7	.808	.971
.270	.035	771	98.3	5.47	.02	6.7	----	.96	1.01	99.8	.827	.994
.281	.024	886	98.2	5.57	.01	5.0	----	.95	.99	99.9	.827	.994
.214	.050	645	96.8	6.03	.08	8.2	----	.95	1.01	99.8	.848	1.019
.268	.032	758	97.2	6.28	.02	4.8	----	.95	1.00	99.9	.885	1.063
.283	.023	877	97.0	6.18	.01	3.4	----	.94	.98	99.9	-----	-----
.202	.058	625	96.4	4.33	.15	20.4	----	.95	1.03	99.5	.857	1.030
.209	.106	493	98.3	8.02	.17	6.6	----	.98	1.12	99.8	.822	.988
.204	.081	603	97.9	8.4	.15	4.3	----	.96	1.08	99.9	.834	1.002
.202	.065	712	98.1	8.4	.02	2.9	----	.96	1.03	↓	.842	1.012
.228	.112	474	97.4	8.8	.03	4.9	----	.99	1.02	↓	.773	.929
.201	.080	610	97.6	9.4	.02	2.9	----	.98	.95	↓	.812	.975
.200	.063	720	97.7	9.5	.02	1.9	----	.94	.94	100.0	-----	----
.204	.081	591	96.8	10.3	.02	2.1	----	.95	----	99.9	.797	.957
.219	.061	718	96.3	10.4	.02	1.3	----	.91	.95	100.0	-----	-----
.223	.106	494	96.8	10.0	.03	3.1	----	.97	.98	99.9	.783	.941
.213	.062	718	96.2	10.9	.01	1.3	----	.92	.96	100.0	-----	-----
.240	.054	692	96.8	12.0	0	1.2	----	.96	.94	100.0	-----	-----
.215	.053	722	96.2	12.1	.01	1.04	----	.96	.93	100.0	.891	1.070
.234	.116	481	97.7	14.8	.18	2.1	----	.96	.98	99.9	.835	1.003
.217	.095	581	98.1	15.5	.01	1.5	----	.97	.96	100.0	.878	1.055
.261	.153	358	98.9	14.8	.02	3.3	----	.97	.99	99.9	.889	1.068
.220	.094	578	96.9	17.0	.01	1.1	----	.97	.96	100.0	.845	1.015
.206	.083	522	100.1	5.4	.41	17.5	----	1.00	.94	99.5	.840	1.009
.233	.054	676	97.4	4.6	.09	15.9	----	.94	.93	99.6	-----	-----
.296	.038	773	96.9	4.6	.03	10.9	----	.96	.93	99.7	.870	1.045
.316	.029	886	98.4	4.8	.01	8.8	----	.97	.94	99.8	.892	1.072
.219	.055	673	97.4	4.5	.1	16.6	----	.96	.91	99.6	.882	1.060

TABLE II. - Concluded.

Run number	Model	Inlet-air conditions: Total pressure, N/cm^2	Total temperature, K	Airflow, kg/sec	Diffuser inlet Mach number	Combustor operating conditions: Reference velocity, V_{ref}, m/sec	Fuel-air ratio	Total pressure loss,	Average outlet temperature, K	Inlet fuel temperature, K	Fuel nozzle differential pressure, N/cm^2	Annulus supplied with fuel	Pattern factor
1459	10-RL2	40.6	477	40.7	0.279	32.0	0.0078	6.77	769	---	---	Both	0.186
1460		40.7	476	40.7	.278	31.9	.0078	6.71	769	---	---		.176
1461		20.5	579	16.4	.243	31.1	.0190	5.65	1248	---	---		.239
1462		20.5	580	16.4	.244	31.1	.0188	5.59	1241	---	---		.253
1482	10-RM1	41.1	479	40.2	.273	31.4	.0122	6.72	927	---	605		.272
1483		20.5	580	16.9	.251	32.0	.0185	6.09	1220	---	239		.329
1484		20.5	583	17.0	.254	32.4	.0184	6.14	1224	294	239		.293
1485		20.7	585		.252	32.2	.0219	6.05	1334	293	340		.364
1486		20.7	586		.253	32.3	.0218	6.17	1325	293	340		.195
1487		20.7	585		.253	32.3	.0217	6.05	1334	292	340		.324
1488		20.9	584		.249	31.8	.0255	5.86	1446	292	470		.396
1489		62.2	587	49.7	.245	31.4	.0059	5.12	814	292	211		.227
1490		62.1	590	49.7	.246	31.7	.0089	5.19	929	291	496		.207
1491		62.1	591	49.7	.246	31.7	.0090	5.23	932	292	499		.205
1492		62.1	592	49.7	.246	31.7	.0106	5.21	987	292	692		.197
1493		62.5	753	38.7	.215	31.3	.0134	3.89	1232	295	692		.230
1494		62.1	759	38.9	.218	31.9	.0134	3.95	1233	297	692		.231
1499		62.3	893	41.4	.255	39.8	.0103	5.40	1249	300	471		.263
1500		62.5	895	41.2	.253	39.5	.0125	5.32	1324	299	696		.268
1501		62.8	899	32.9	.199	31.6	.0104	3.33	1254	304	298		.282
1502	10-RM1	62.7	895	33.2	.201	31.9	.0103	3.40	1253	303	298		.293
1503		62.0	897	33.3	.204	32.4	.0137	3.51	1360	300	532		.291
1504		61.9	897	33.4	.205	32.4	.0154	3.55	1417	299	689		.282
1505		62.5	899	24.9	.150	24.1	.0104	1.92	1255	310	170		.315
1506		41.0	482	40.0	.273	31.5	.0123	6.71	938	292	600		.307
1507		40.9	481	40.1	.274	31.6	.0123	6.62	939	292	609		.314

[a] $\frac{NO_{x_a}}{NO_{x_c}} = \frac{NO_x\text{(actual)}}{NO_x\text{(calculated (from } NO_{x(std)}\text{))}}$.

EXPERIMENTAL DATA

Stator factor	Rotor factor	Combustor performance characteristics										
		Combustor average temperature rise, K	Thermocouple combustion efficiency, percent	NO_x emission index, g/kg of fuel	HC emissions index, g/kg of fuel	CO emission index, g/kg of fuel	Smoke number	FARR	FARRO	Gas analysis combustion efficiency, percent	$NO_{x(std)}$	NO_{x_a}/NO_{x_c} [a]
0.322	0.186	292	95.8	1.40	21.3	81.5	----	0.96	0.97	96.0	----	-----
.312	.187	293	96.1	1.46	22.5	88.4	----	1.00	1.02	95.7	----	-----
.246	.068	669	99.5	2.45	.22	16.5	----	.92	1.00	99.6	----	-----
.249	.069	660	98.9	2.83	.14	11.7	----	.95	1.08	99.7	0.851	1.022
.300	.106	447	97.1	1.4	13.7	76.9	----	.93	1.00	96.8	----	-----
.329	.067	639	97.2	2.3	.2	23.9	----	.94	.98	99.4	----	-----
.295	.067	640	97.8	2.8	.09	21.0	----	1.00	1.03	99.5	.857	1.030
.364	.048	749	98.0	2.9	.07	7.6	----	.86	1.04	99.8	----	-----
.216	.057	739	96.9	2.9	.07	7.7	----	.95	1.04	99.8	.810	.973
.324	.047	749	98.6	3.2	.11	7.8	----	.95	1.07	99.8	.892	1.072
.396	.029	862	98.6	3.4	.11	4.7	----	.96	1.08	99.9	.868	1.043
.385	.245	227	99.5	4.5	4.7	31.0	----	1.00	1.14	98.8	----	-----
.307	.166	338	101.1	4.5	1.9	21.9	----	.93	1.07	99.3	----	-----
.300	.166	340	101.1	4.9	1.2	20.3	----	.99	1.13	99.4	.753	.905
.298	.139	395	101.0	5.2	.65	18.0	----	.96	1.13	99.5	.793	.953
.286	.124	479	102.4	9.5	.05	2.1	----	.89	.99	99.9	----	-----
.299	.128	474	101.4	11.0	.04	2.0	----	1.00	1.11	99.9	.864	1.038
.349	.182	355	100.5	16.2	.07	1.37	----	1.02	1.13	100.0	.754	.906
.323	.154	429	101.0	16.3	.04	.76	----	1.04	1.12		.824	.990
.345	.179	355	100.1	18.7	.05	.61	----	1.08	1.15		----	-----
.349	.178	358	101.4	17.9	.06	.66	----	1.00	1.09		.823	.989
.331	.142	462	100.9	18.2	.04	.94	----	.97	1.07		.830	.997
.330	.126	520	100.9	18.8	.04	.70	----	.96	1.06		.852	1.024
.427	.177	356	99.5	20.5	.05	1.00	----	1.01	1.08		.879	1.056
.326	.096	456	97.9	2.1	14.6	76.5	----	.93	.97	96.7	----	-----
.313	.095	457	98.3	2.1	7.3	58.1	----	.93	.98	97.9	----	-----

TABLE III. - DOUBLE-ANNULAR RAM-INDUCTION

COMBUSTOR DIMENSIONS AND SPECIFICATIONS

Length, cm	
Compressor exit to turbine inlet	51.1
Fuel nozzle face to turbine inlet	30.5
Diameter, cm	
Inlet outside	80.77
Inlet inside	71.1
Outlet outside	89.9
Outlet inside	69.9
Shroud diameter, cm	
Outside	94.2
Inside	57.2
Reference area (between shrouds), cm^2	4270
Diffuser inlet area, cm^2	1177
Open hole area (including cooling), cm^2	1571
Flow spreader inlet area, cm^2	
Outside diameter passage	348
Center passage	785
Inside diameter passage	339
Exit area, cm^2	2503
Number of fuel nozzles and swirlers	64
Number of diffuser struts	16
Number of ram-induction scoops	256
Rows, primary zone	1
Rows, secondary zone	1
Ratio length to annulus height	
Outer annulus	4.8
Inner annulus	3.9

TABLE IV. - SCOOP AREAS[a] AND SIZES FOR

DOUBLE-ANNULAR RAM-INDUCTION COMBUSTOR[b]

Type of scoop	Discharge area, cm^2	Length, cm	Width, cm
Outer liner primary	------	-----	-----
Outer liner secondary	------	2.637	2.591
Outer center shroud primary	122.85	1.981	1.938
Outer center shroud secondary	109.03	1.295	3.407
Inner center shroud primary	122.85	1.981	1.938
Inner center shroud secondary	109.03	1.295	3.407
Inner liner primary	122.35	2.07	1.847
Inner liner secondary	219.25	3.31	2.07

[a]All areas are actual area for full annulus.

[b]See fig. 1.

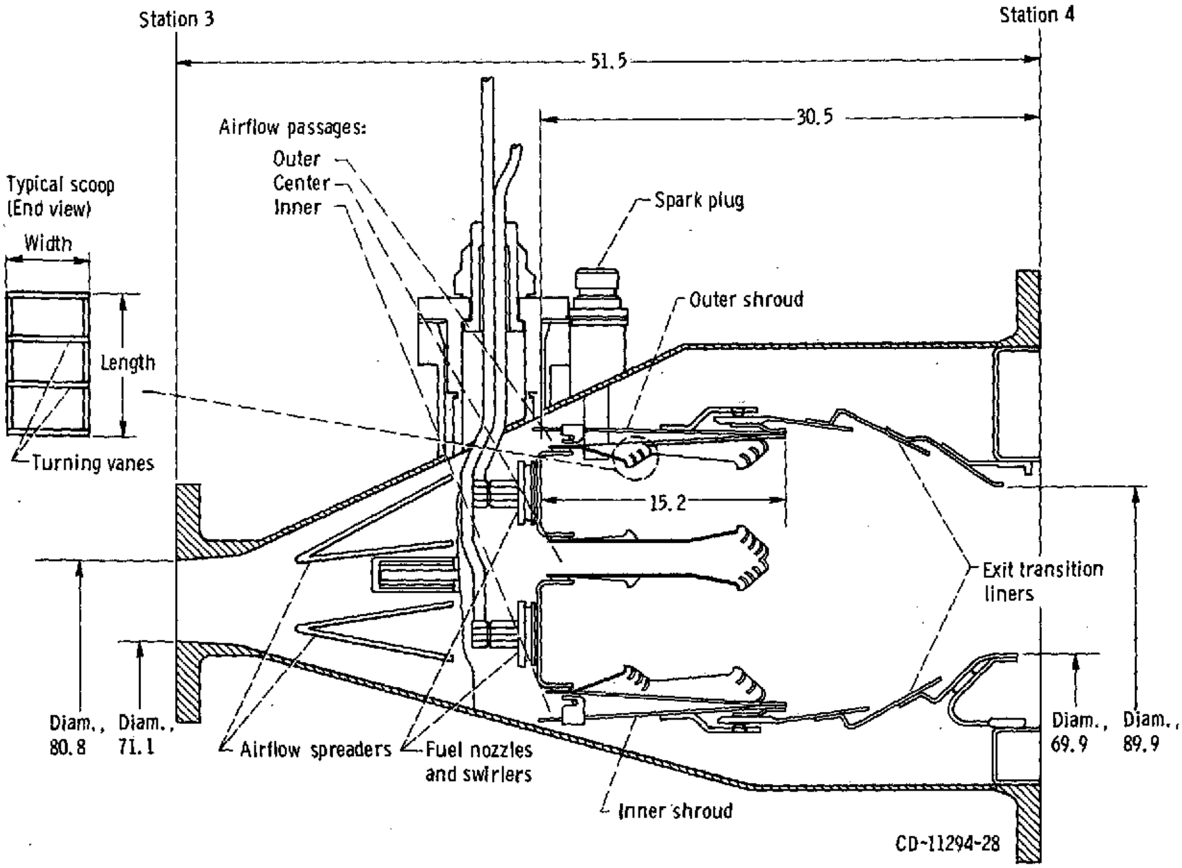

Figure 1. - Cross section of double-annular ram-induction combustor. (All dimensions are in cm.)

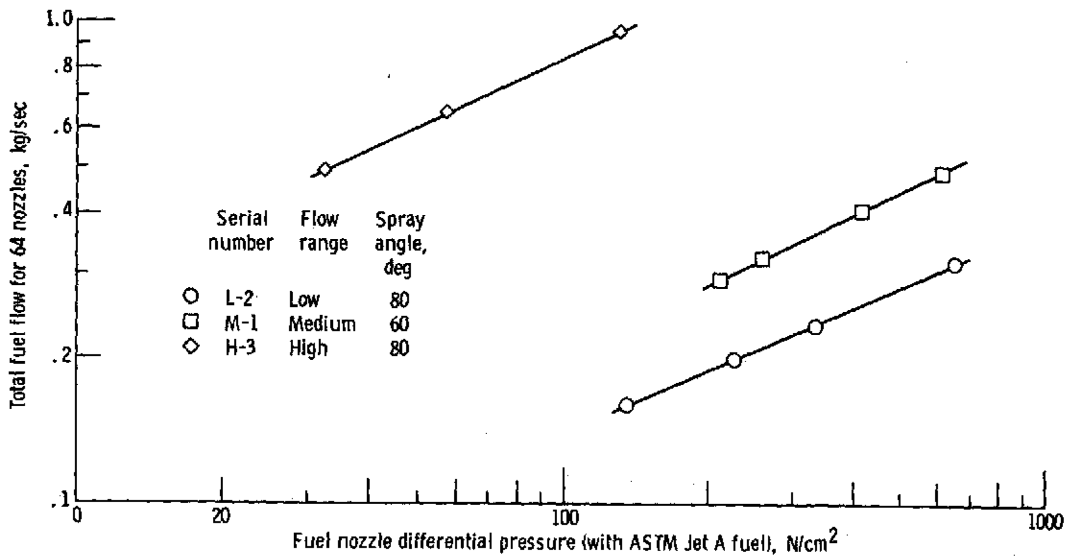

Figure 2. - Fuel flow plotted against fuel nozzle differential pressure for all fuel nozzles tested.

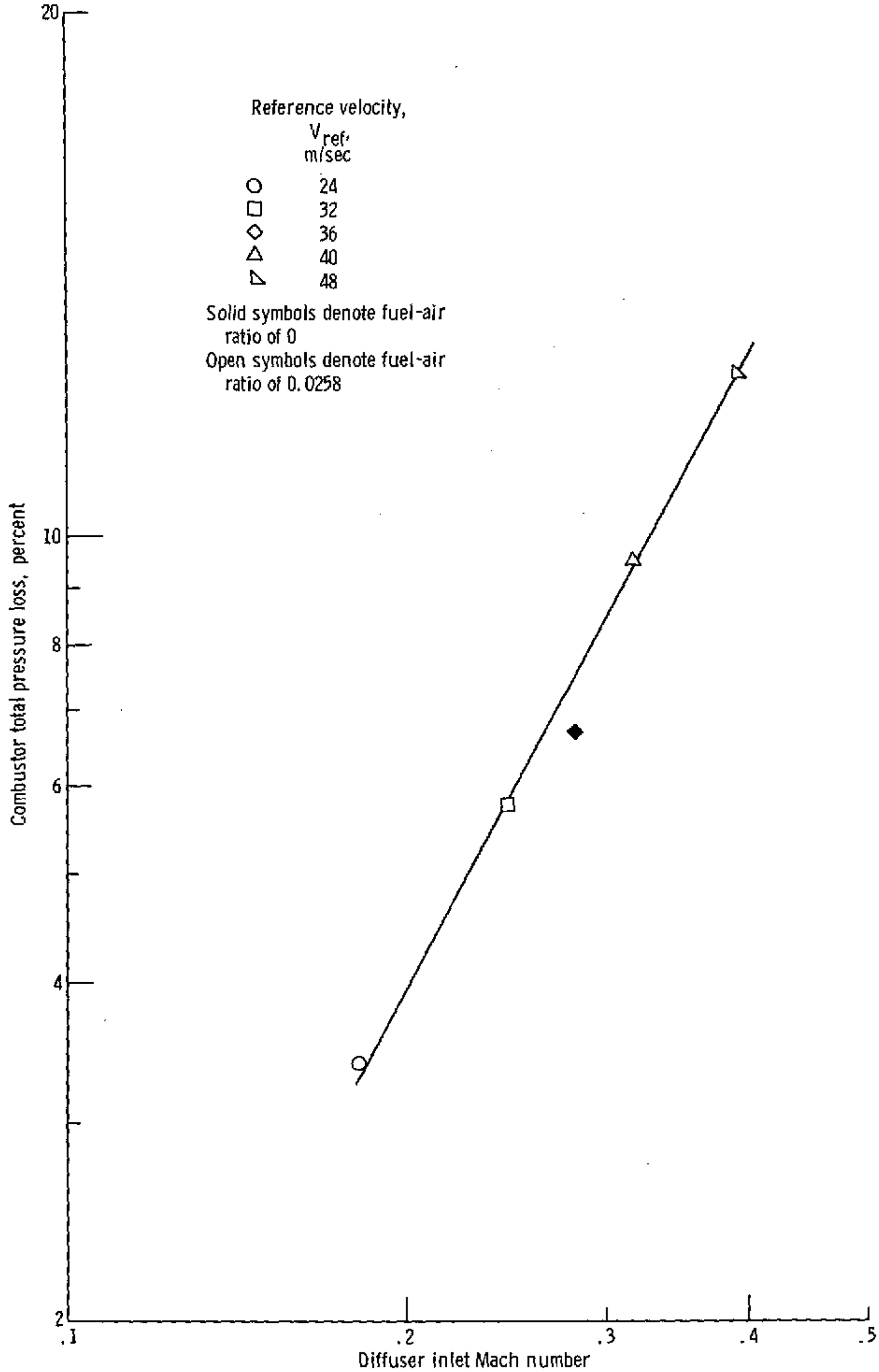

Figure 3. - Combustor total pressure loss as a function of diffuser inlet Mach number. Inlet air temperature, 590 K; inlet total pressure, 62 newtons per square centimeter.

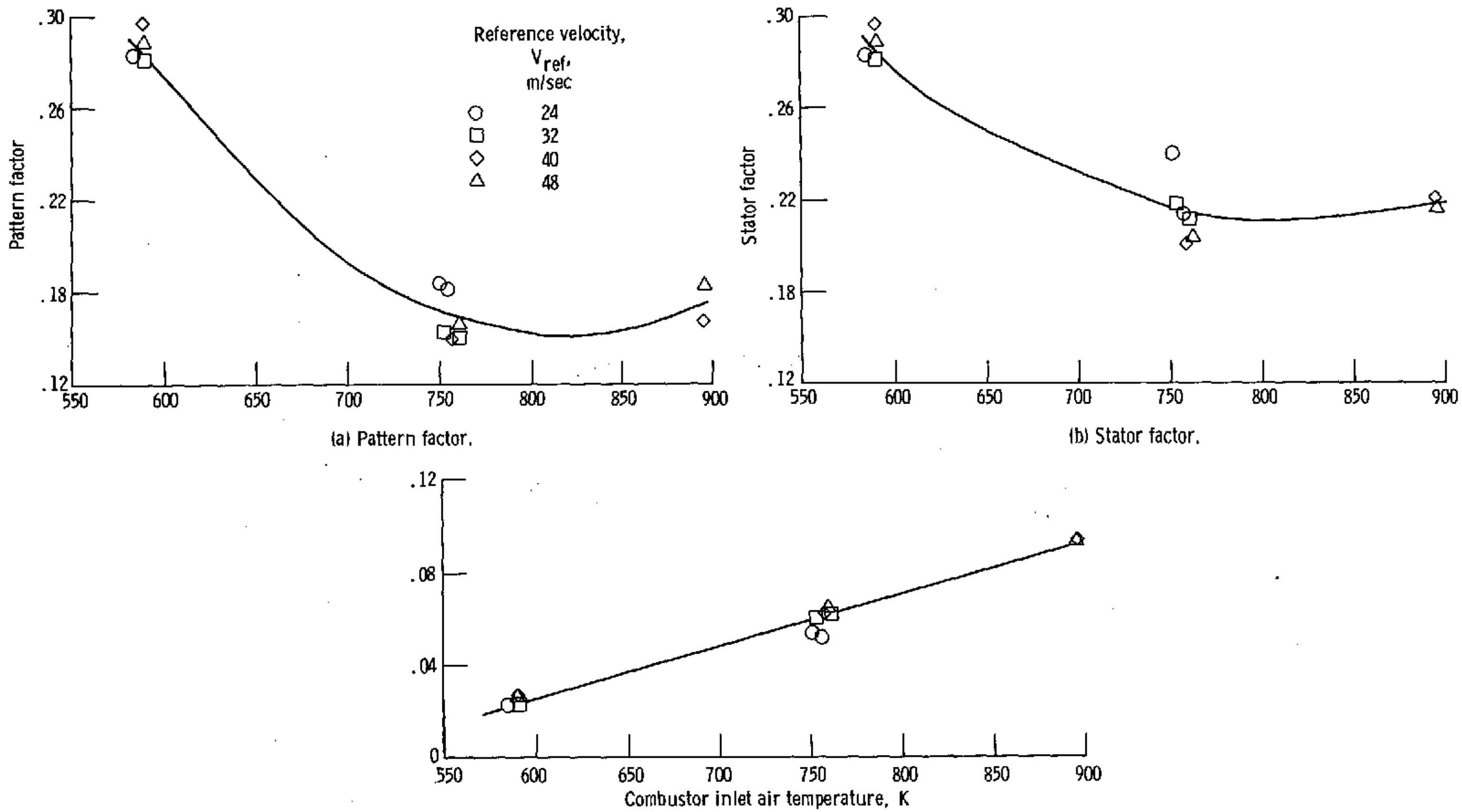

(a) Pattern factor.

(b) Stator factor.

(c) Rotor factor.

Figure 4. - Combustor exit temperature parameters as a function of inlet air temperature. Inlet total pressure, 62 newtons per square centimeter; average exit temperature, 1475 K.

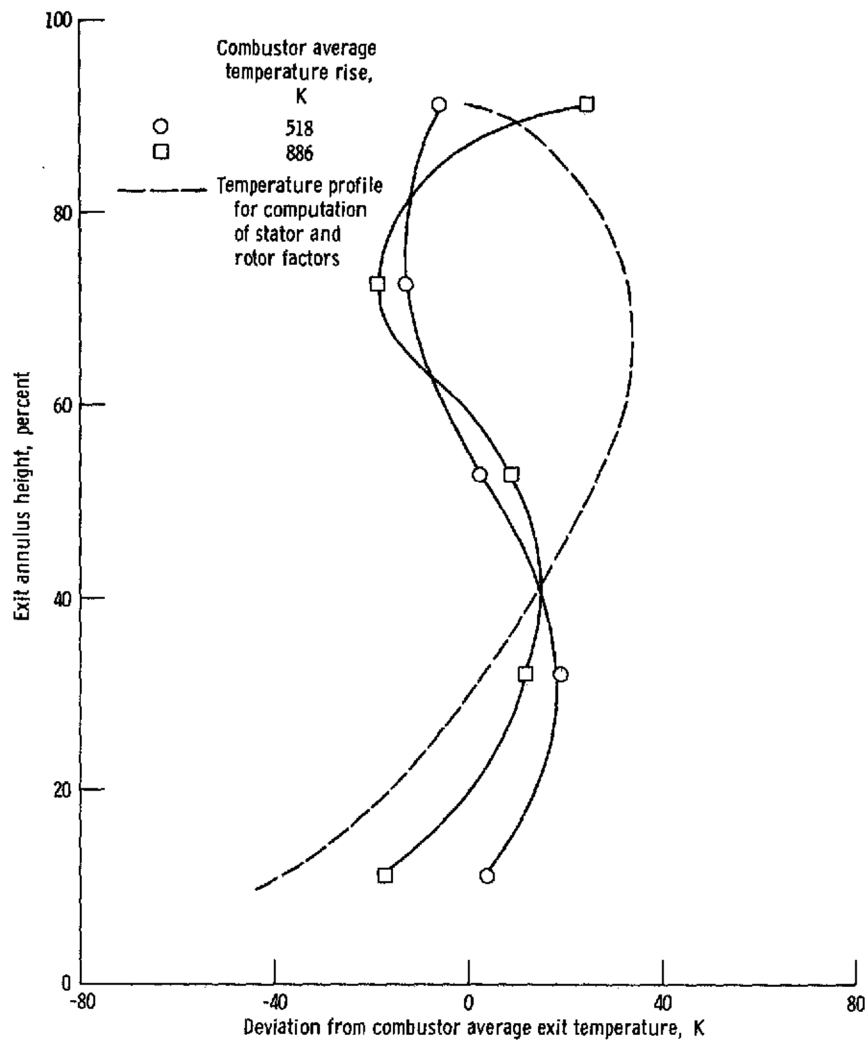

Figure 5. - Variation of exit average radial temperature profile with combustor average temperature, 585 K; inlet total pressure, 62 newtons per square centimeter; reference velocity, 32 meters per second.

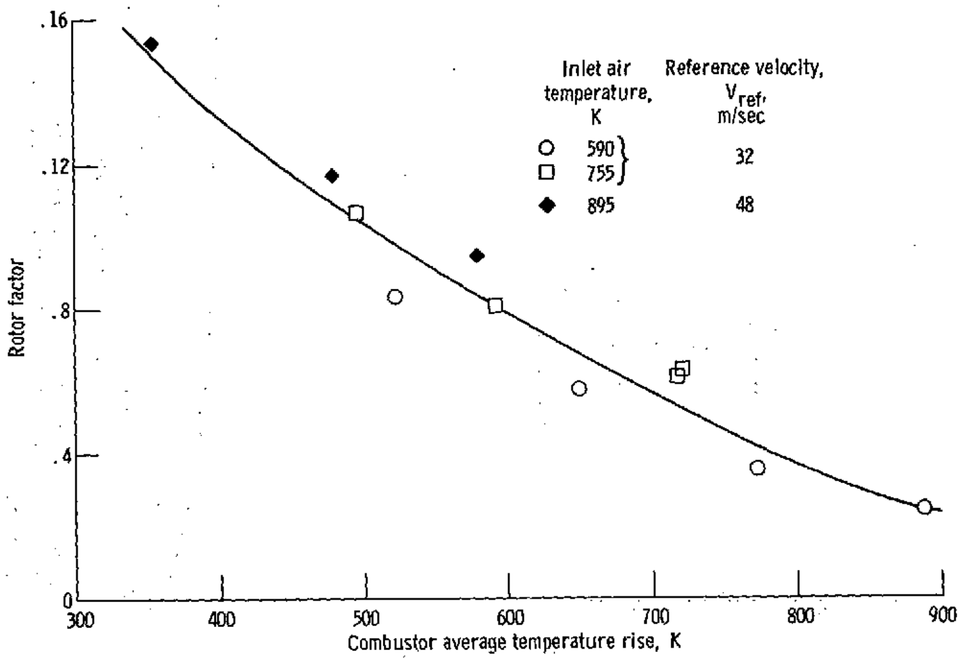

Figure 6. - Rotor factor as a function of combustor average temperature rise showing effect of inlet air temperature.

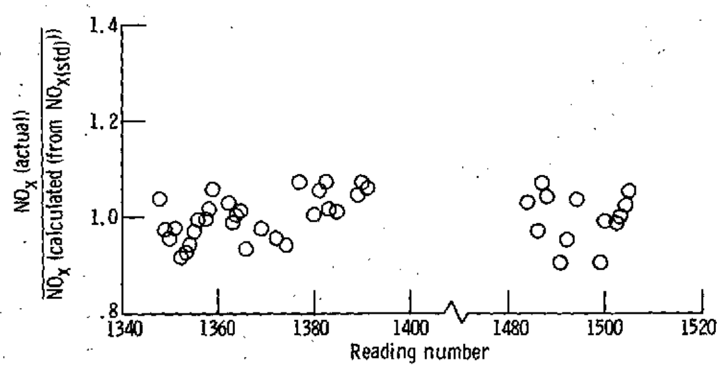

Figure 7. - Equation verification of actual NO_x value over computed NO_x value using $NO_{x(std)} = 0.832$.

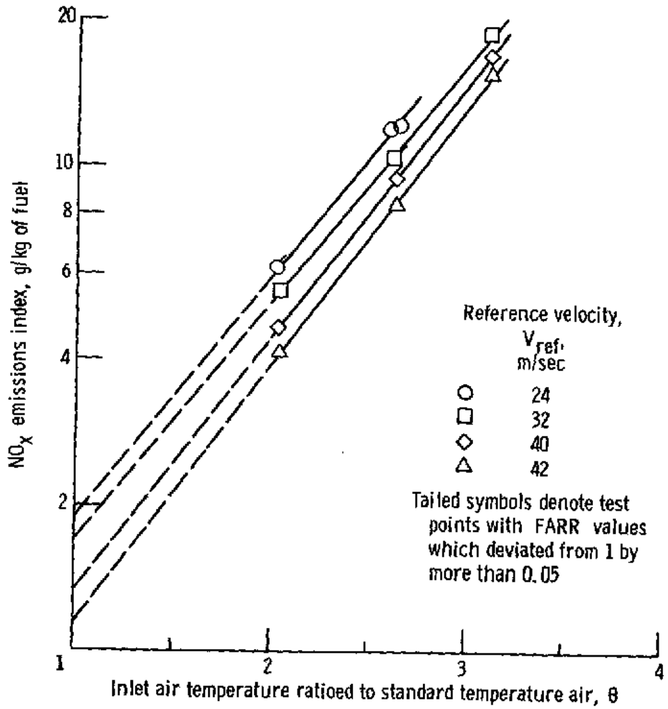

Figure 8. - NO_X emissions index as a function of inlet air temperature showing effect of reference velocity. Inlet total pressure, 62 newtons per square centimeter; exit average temperature, 1470 K.

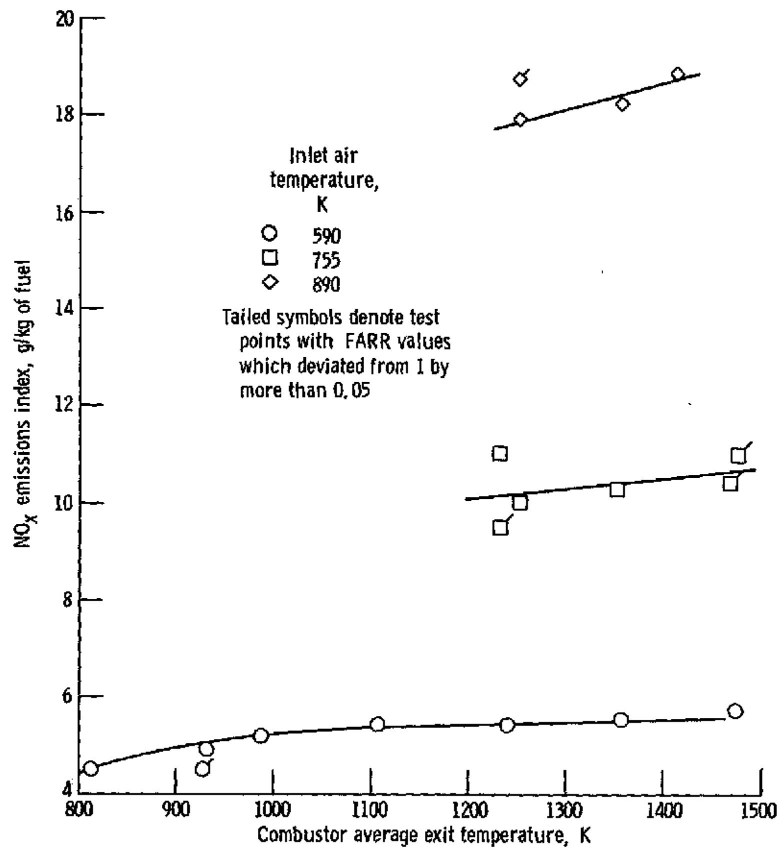

Figure 9. - NO_X exhaust emissions index as a function of combustor average exit temperature showing effect of inlet temperature. Reference velocity, 32 meters per second.

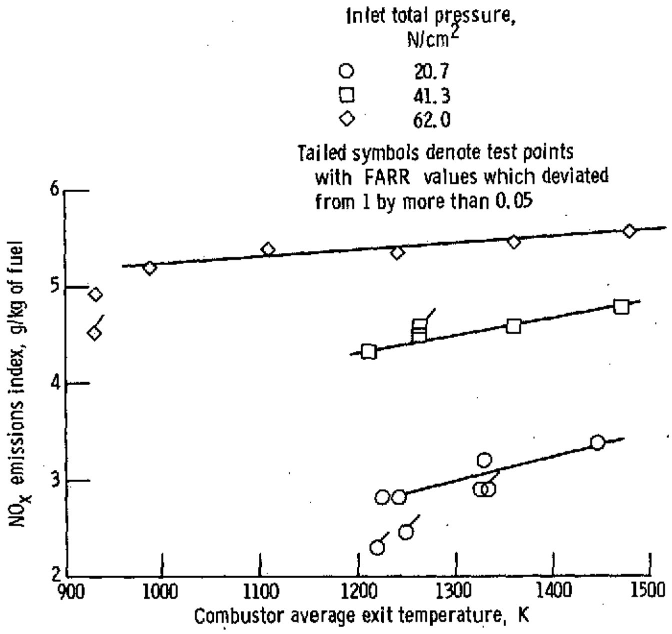

Figure 10. - NO_x exhaust emissions index as a function of combustor average exit temperature showing the effect of inlet total pressure. Inlet air temperature, 590 K; reference velocity, 32 meters per second.

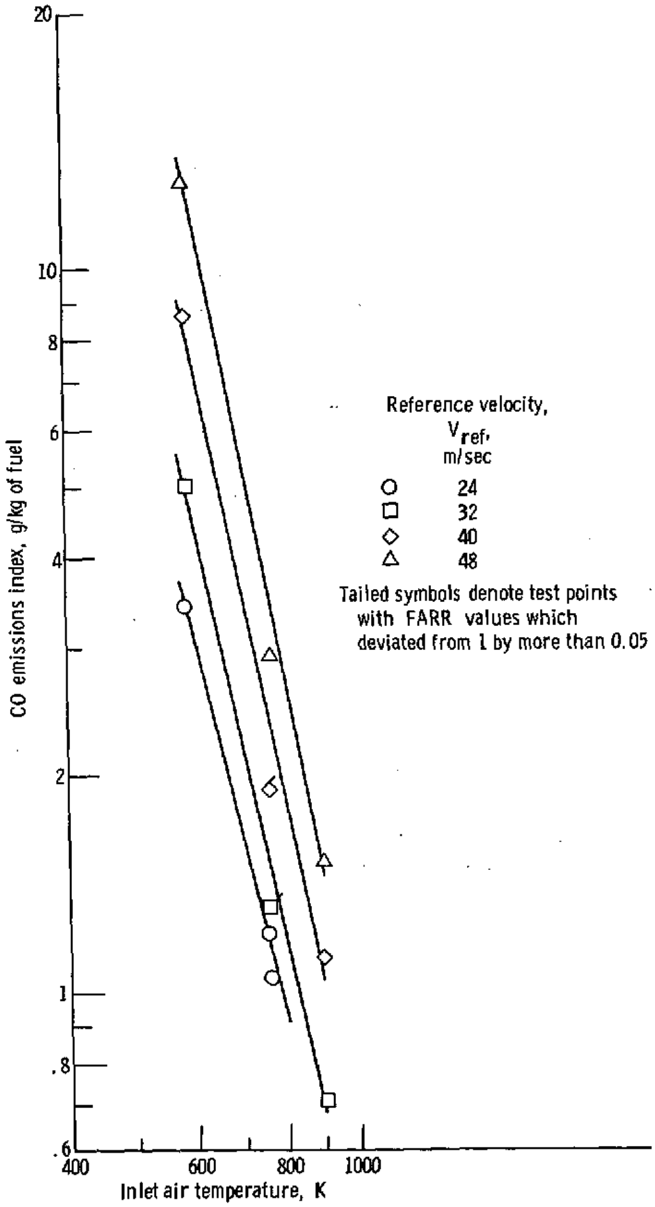

Figure 11. - Effect of inlet air temperature and reference velocity on CO emissions index. Inlet total pressure, 62 newtons per square centimeter; exit average temperature, 1470 K.

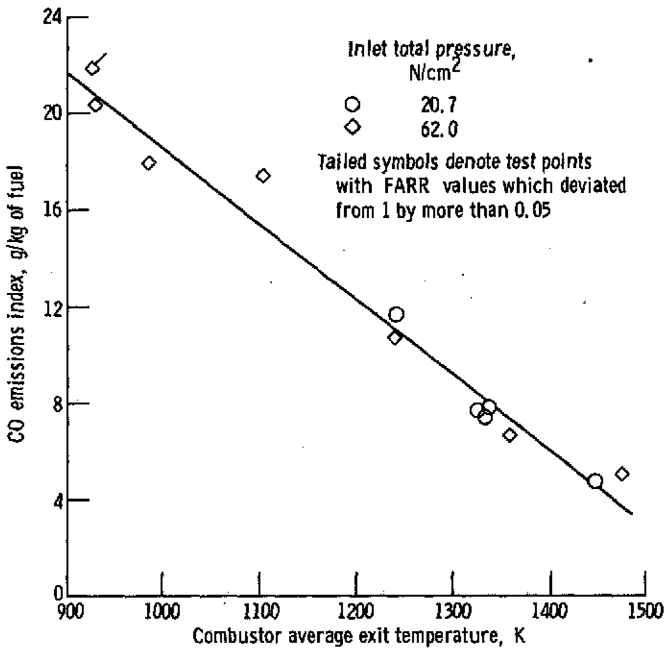

Figure 12. - Carbon monoxide emissions as a function of combustor average exit temperature showing effect of inlet total pressure. Inlet air temperature, 590 K; reference velocity, 32 meters per second.

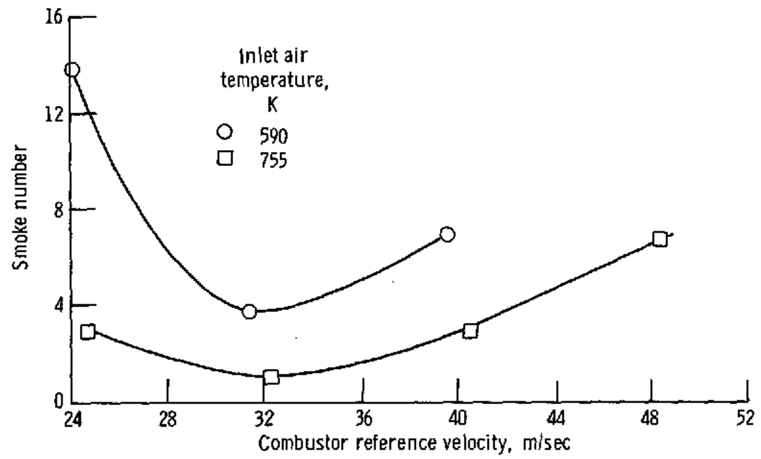

Figure 13. - Smoke number as a function of reference velocity showing effect of inlet air temperature. Inlet total pressure, 62 newtons per square meter; exit average temperature, 1475 K.

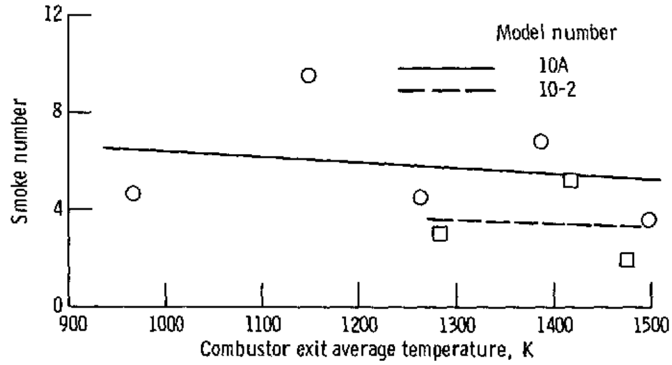

Figure 14. - Smoke number as a function of combustor exit average temperature. Inlet air temperature, 590 K; inlet total pressure, 62 newtons per square centimeter; reference velocity, 32 meters per second.

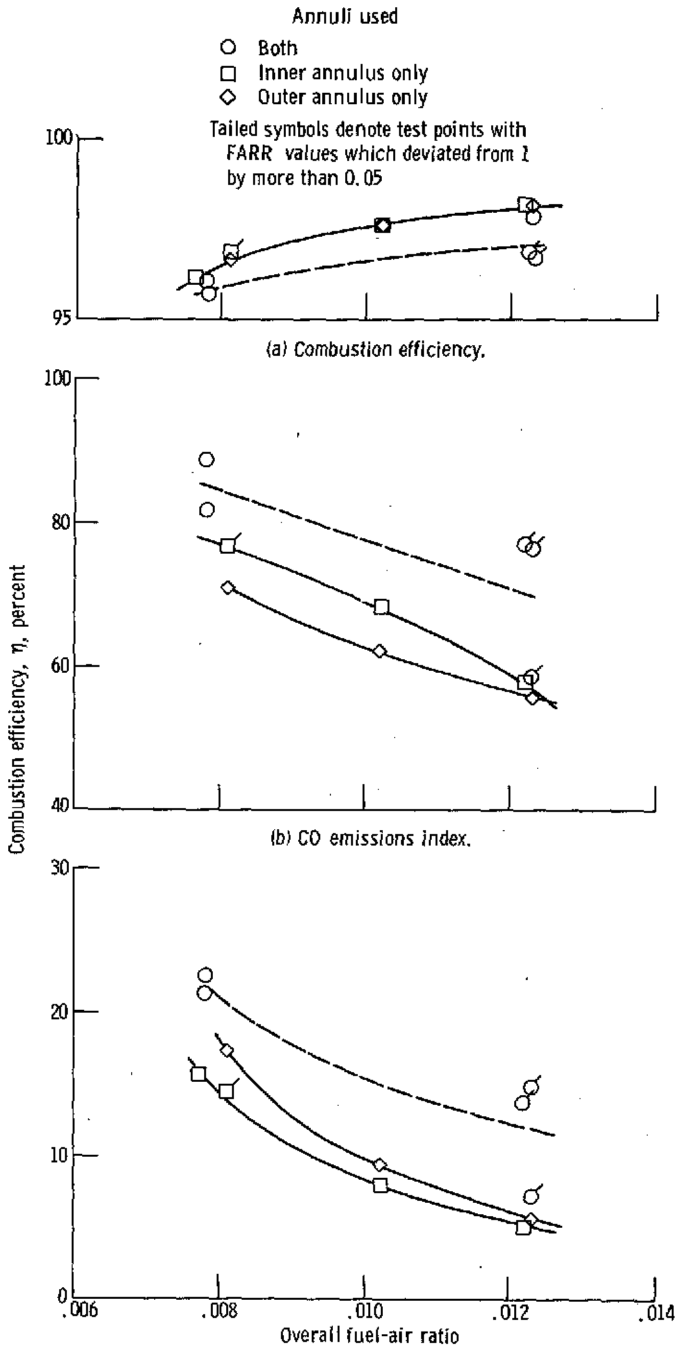

(c) Hydrocarbons emissions index.

Figure 15. - Combustor performance at high idle conditions of 495 K inlet air temperature, 41-newton-per-square-centimeter inlet total pressure, and 31.4-meter-per-second reference velocity showing effect of radial fuel staging. Three different flow ranges of fuel nozzles were used to optimize fuel atomization.

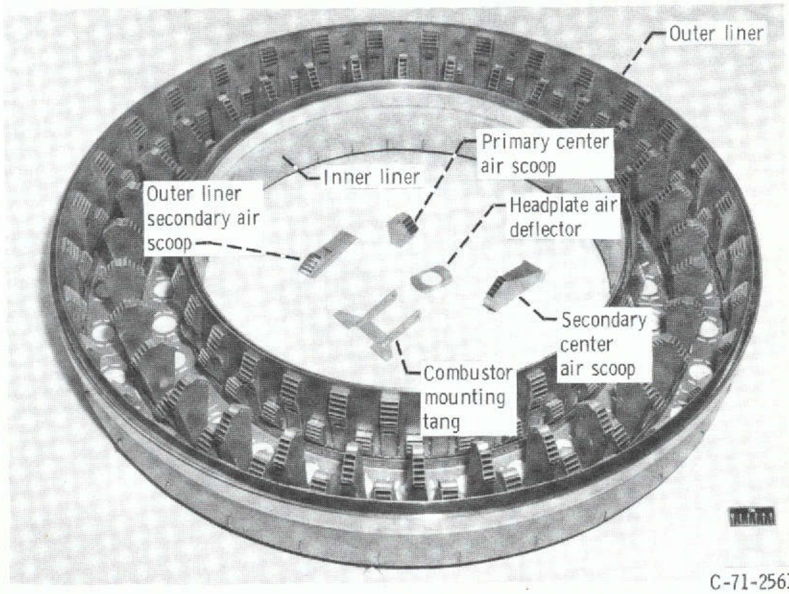

(a) Viewed from downstream (fuel nozzles, headplate air deflectors, and transition liners removed).

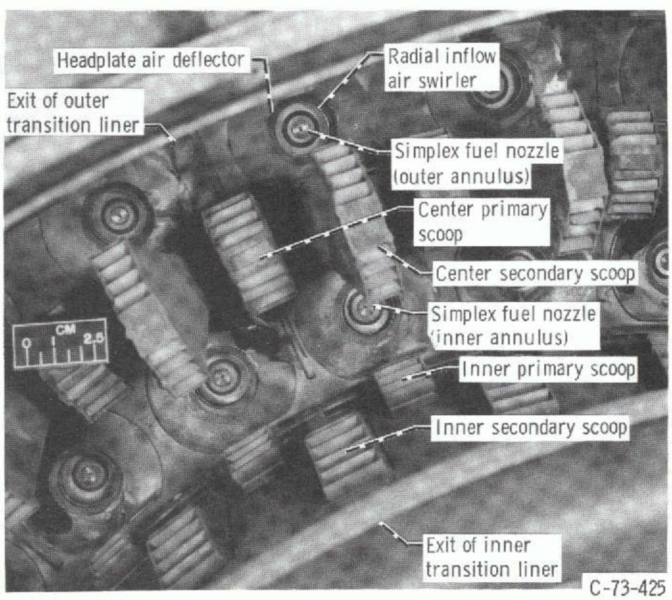

(b) Closeup view.

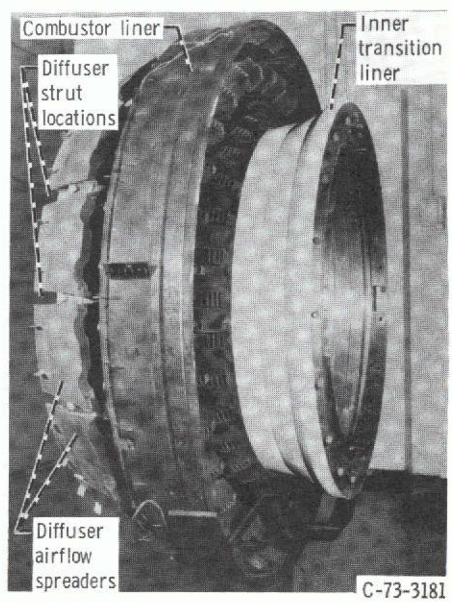

(c) Side view (outer transition liner removed).

Figure 16. - Double-annular ram-induction combustor.

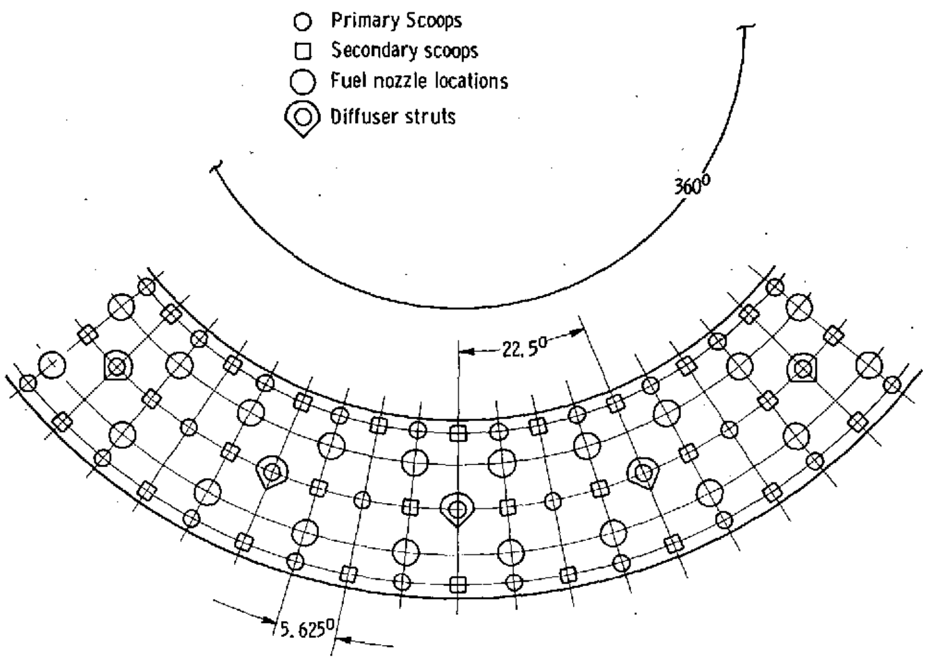

Figure 17. - Circumferential arrangement of combustor scoops and fuel nozzles.

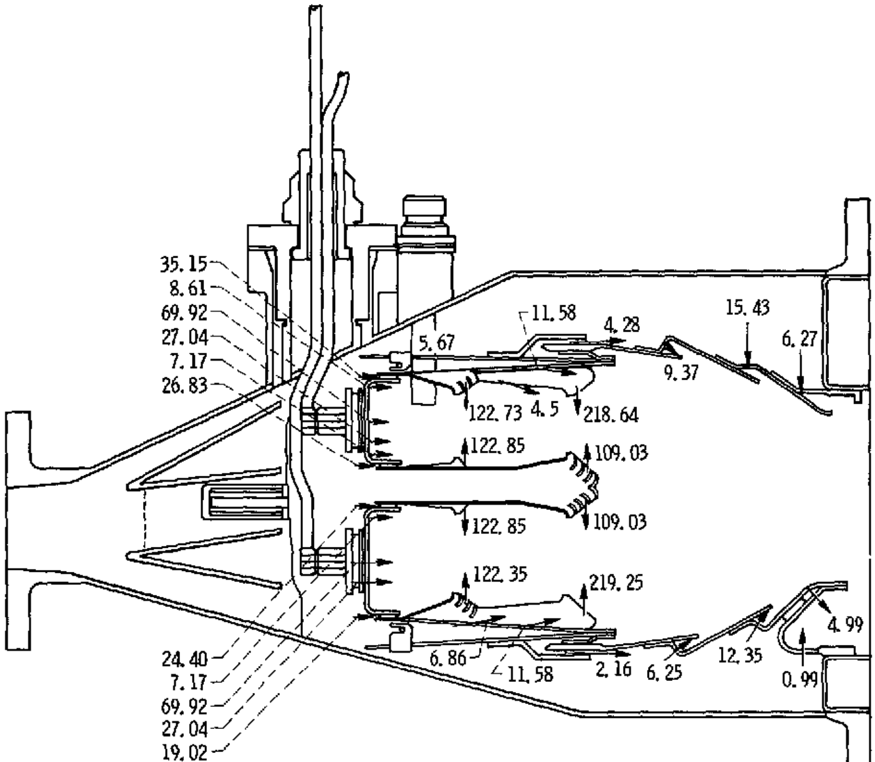

Figure 18. - Effective flow area distribution for double-annular ram-induction combustor. Swirler discharge coefficient, 0.50; hole discharge coefficient, 0.62; scoops and slot discharge coefficient, 1.00; total area (effective), 1571 square centimeters. (All areas are based on a full annulus with units of cm^2.)

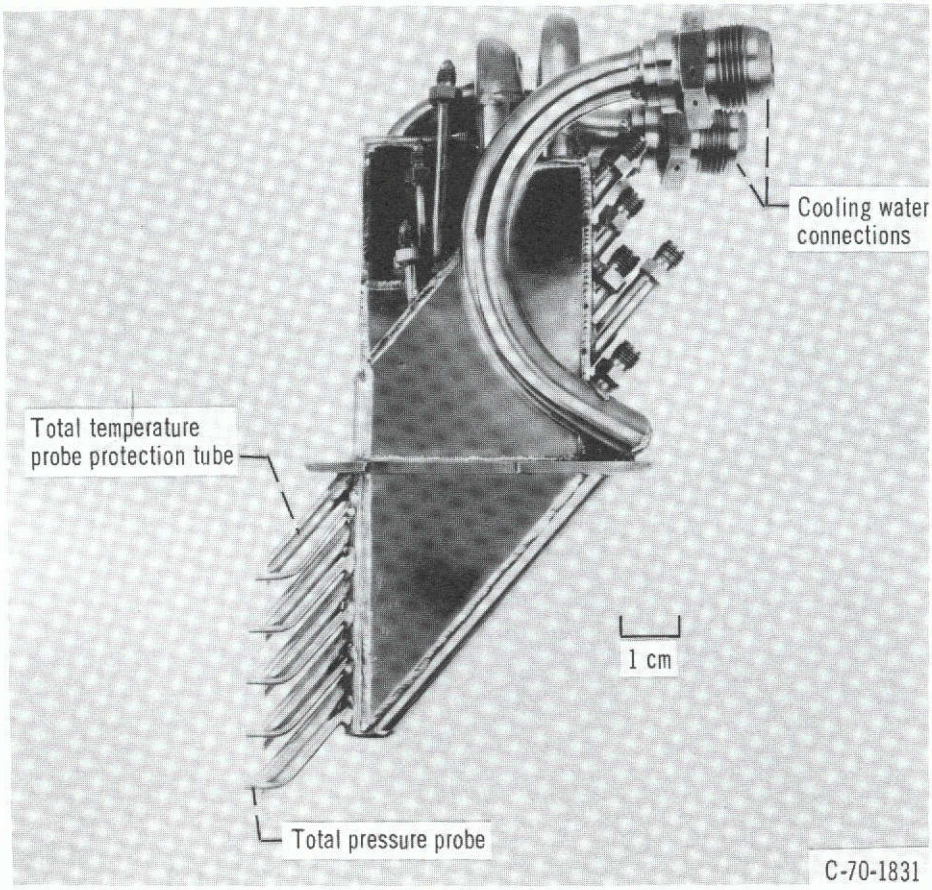

Figure 19. - Five-point total temperature and total pressure water-cooled probe assembly.

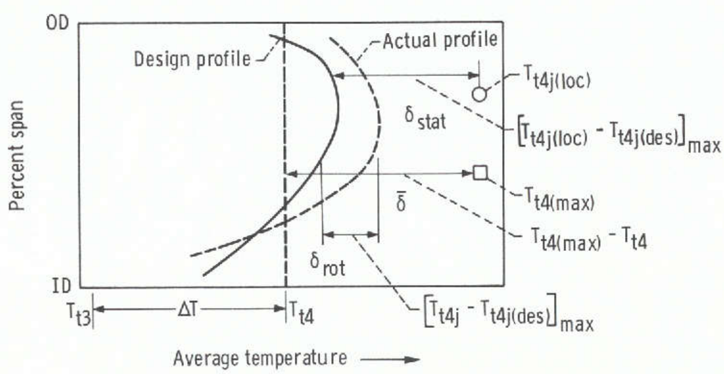

Figure 20. - Explanation of terms in exit temperature profile parameters.